

Shear and Thermal Testing of Adhesives for VELO Upgrade

A Sticky Study

S. de Capua¹, J. Freestone¹, S. Klaver¹, C. Parkes¹,
P. Rodriguez¹, A. Shtipliyski¹, G. Stelmasiak¹

¹*University of Manchester*

Abstract

As part of the R&D process of the LHCb VELO Upgrade, a study has been performed on the thermal and mechanical performance of the adhesives Stycast 2850FT, 3M 9461P, and Araldite 2011. One or more of these adhesives could be used to attach the ASICs and hybrids to the microchannel cooling substrate. Samples were irradiated at up to the maximum dose expected at the upgrade. Shear tests of the samples were made and a suitable performance obtained from all glues. Some failures were encountered with Stycast 2850FT glued samples and this is attributed to the sample preparation. The relative thermal conductivities of the adhesives were also determined by measuring the relative temperature difference across a glued joint while one side is heated.

Contents

1	Introduction	1
1.1	Proposed Adhesives and General Considerations	2
2	Shear test	3
2.1	Sample preparation	3
2.1.1	Materials cutting	3
2.1.2	Adhesive deposition	4
2.1.3	Carrier plates attachment	4
2.1.4	Irradiation	6
2.2	Apparatus	6
2.2.1	LVDT	7
2.2.2	Load cell	8
2.3	Calibration	8
2.3.1	Load Cell Calibration	8
2.3.2	LVDT Calibration	10
2.3.3	Temperature Correction	10
2.4	Results	11
2.5	Notes on the Methods	13
3	Thermal studies	15
3.1	Introduction	15
3.2	Test Setup	15
3.3	Results	16
4	Conclusions	19
A	Shear force test procedure	20
A.1	Procedure for gluing samples	20
A.2	Procedure for shear force testing	20
B	Thermal test procedure	21
C	Specifications of the Irradiation	22
	References	22

1 Introduction

The LHCb VELO will be upgraded during LHC Long Shutdown 2 [1]. The VELO modules will be completely redesigned to accommodate 4 pixel tiles per module, each tile made of three ASICs bump-bonded to a silicon sensor. The tiles will be glued onto a silicon substrate, which provides both the cooling and the mechanical support for the sensors and the FE electronics. The heat generated will be removed by bi-phase CO₂ coolant circulating at -30 °C through microchannels etched inside the 400 μm thick silicon substrate. Additional advantages of the microchannel cooling are a perfect CTE match with the silicon ASICs and a reduced material budget. A cross-section of the module design is shown in Fig. 1.

The detector will operate in a radiation environment for up to ten years. The experiment is expected to collect an integrated luminosity of 50 fb^{-1} , for which the inner regions of the sensors will receive a dose of $8 \times 10^{15} \text{ MeV n}_{\text{eq}}/\text{cm}^2$ or 400 MRad.

The readout ASICs, called the VeloPix, closest to the interaction region will have the highest bandwidth requirements, generating up to 3 W of heat. The leakage current in the sensors after irradiation will reach $200 \mu\text{A}/\text{cm}^2$ at 1000 V, generating 1 W of heat. In total, the cooling of the VELO upgrade must be capable of dealing with up to 36 W per module, while keeping a low material budget. The components on the hybrid circuit that draw significant electrical (such as the GBT chip indicated in Fig. 1) must also be effectively cooled.

The VELO modules are operated in vacuum. Consequently, the glue which attaches the FE electronics to the microchannel plate plays a crucial role as it is the only interface between the heat sources and the cooling plate.

Additional constraints are the required precision during the gluing of the sensor tiles, which should be less than 10 μm . The attachment of the Kapton readout hybrid circuit to the substrate is also required although with relaxed requirements on the precision relative to that required for the sensor tiles. The hybrid must be securely glued in the relevant area to the substrate to allow the bump-bonding between the hybrid and the readout ASIC to be performed.

These requirements lead to the necessity to identify adhesives with good mechanical and thermal properties for operation in vacuum, elevated radiation levels and working temperatures down to -30 °C. This document describes tests performed on the mechanical and thermal properties of thermally conductive adhesives that are considered for use in the modules.

The glues that have been tested are described in Sect. 1.1. A shear test apparatus was designed to measure the shear stress the glued samples can undergo before either they break or move, the apparatus and results are described in Sect. 2. The thermal conductivity measurements that were performed on the samples are described in Sect. 3. A conclusion and outlook are given in Sect. 4.

Adhesive	Mixing ratio	Curing schedule	Pot life	Shelf life
Araldite 2011 [2]	100:100 by volume	10 h @ 23°C	100 mins	36 months
Stycast 2850 FT [3]	100:3.5 by mass	24 h @ 25°C	45 mins	12 months
3M 9461P 30 μm [4]	-	-	-	18 months

Table 1: Summary of the properties of the adhesives studied with focus on the ones relevant for their preparation and handling.

2 Shear test

In order to measure the mechanical properties of the different glues a shear test setup was built. The samples were subjected to shear forces and the displacement between the two glued layers was measured with micron precision. In this section the preparation of the samples is described in Sec. 2.1, following by the description of the devices used to measure the forces and the displacements in Sec. 2.2. Next the procedures followed to calibrate the apparatus are explained in Sec. 2.3 and finally the results are presented in Sec. 2.4.

2.1 Sample preparation

Ten samples were prepared for each adhesive, five of which were irradiated. Each of the produced samples were given a unique ID to track the details of the assembly procedure and to correlate those to any specific behaviour during testing. For this purpose a naming convention was adopted where the ID would include a letter and number. The letter would indicate the name of the adhesive and the number, the order in which the sample was created. For example S2 is the second sample created with the Stycast adhesive. The non-irradiated samples were used to test the procedures and practice using the apparatus; the results in this note are from the irradiated samples only.

In the prototyping stage, samples were produced from 300 μm thick glass tiles using various adhesives. The material was selected for its close mechanical properties to silicon and that its transparency made it possible to observe the glue deposition before and after curing. This allowed the different stages of the production process to be tuned to the various properties of the adhesives and to ensure that the necessary steps are taken to properly handle the adhesives during production of the samples.

2.1.1 Materials cutting

A sample size of $15 \times 16 \text{ mm}^2$ was selected as it is similar to the size of a single ASIC pixel module for the VELO upgrade. Sample tiles were made from silicon wafers in order to probe silicon on silicon bonding as required in the modules.

The silicon tiles were cut from a standard 6" wafer of 400 μm thickness and polished on one side. The wafer was cut in two stages: first it was cut with a diamond saw into 15 mm wide strips. Then, each strip was further cut into tiles of $15 \times 16 \text{ mm}^2$ using a diamond pen. Using this process, a total of 130 silicon tiles were produced with average dimensions of $x = (15.2 \pm 0.3) \text{ mm}$ and $y = (16.2 \pm 0.4) \text{ mm}$.

2.1.2 Adhesive deposition

The Araldite and Stycast adhesives are in the form of an epoxy-based two-component solution. This requires a proper mixing in order to achieve the nominal bond strength, but care must be taken for the adhesives to be free from air bubbles. To address this issue and ensure consistency in the preparation of the adhesives for testing, a mixing robot was utilised for the assembly of the two-component adhesives. The robot used was SpeedMixer DAC 150.1 FVZ-K and the mixing procedure involved operating the machine for 4 minutes at 2600 rpm.

The 3M tape came prepared from the manufacturer. In practice, the tape never cures and for optimal performance the manufacturer recommends that it is thermally cycled before maximum adhesive strength is achieved. The manufacturer's recommendations were followed and the samples cycled four times in a climate chamber through: 4 hours at 70 $^{\circ}\text{C}$; 4 hours at $-29 \text{ }^{\circ}\text{C}$; 16 hours at 25 $^{\circ}\text{C}$; comprising ~ 100 hours in total.

An automated glue deposition system was used for the liquid glues. The robot consists of a moveable glue deposition head and a table onto which the material to be glued is placed. It was programmed to release adhesive in a rectangular pattern using a 5×5 grid of dots¹. An image of the deposition pattern is shown in Fig. 2. The program allows for adjusting the x , y and z coordinates, as well as for controlling the time spent at each point and the amount of glue released. The latter two are important parameters to tune if the viscosity of the test adhesives varies. For the adhesives selected in the current study, the viscosity was similar such that no adjustments of those parameters were required.

For all test samples the glue was deposited on the polished side of a silicon tile for consistent preparation. Those tiles were placed in the machine on top of the working table and were held stationary using strips of Kapton. To ensure accurate positioning a custom printed grid was placed underneath the sample to ensure consistent alignment for all. This grid is also shown in Fig. 2.

2.1.3 Carrier plates attachment

To test samples with the shear testing apparatus, it was necessary to attach the glued sample tiles to larger aluminium carrier plates. This was done using the Araldite 2011 adhesive as it has been identified as the strongest available at the time of the study. The attachment was done by applying glue on both carrier plates in between which the

¹After this study was finalised, the University of Manchester bought a Fisnar FN2000 glue robot, which will be the robot to be used during the production of the modules and it allows depositing dots and lines of glue.

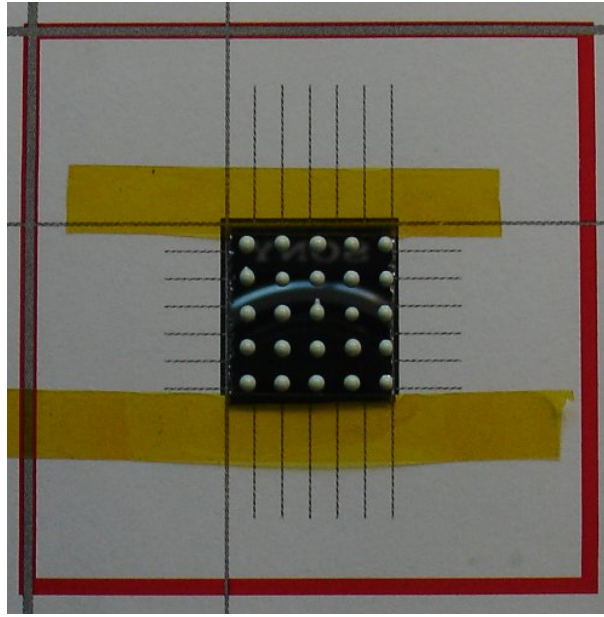


Figure 2: A picture of a $15 \times 16 \text{ mm}^2$ silicon sample tile attached onto the glue deposition pattern. The glue is deposited in a square grid. The tile is attached to the glue robot worktable via strips of Kapton, allowing for a margin of at least 2 mm on each side. Strips of Kapton are left attached to the Si tile to act as a separator of $60 \mu\text{m}$ thickness.

sample tile is placed. A schematic of the attachment of silicon samples, carrier plates and glue is shown in Fig. 3. To deposit the glue, the same machine program is used with a modification to allow for the larger height of the aluminium plates and the slightly larger amounts of glue deposited.

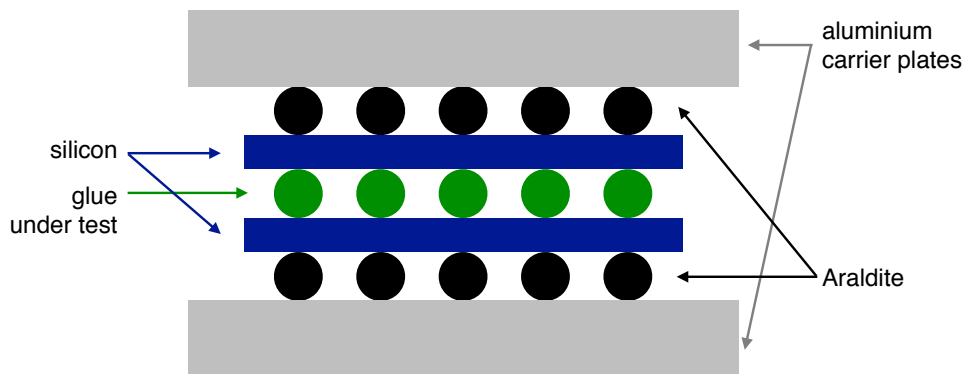


Figure 3: A schematic of the attachment of the carrier plates to the silicon-glue sandwich.

Afterwards, the sample was placed in the centre of the carrier plate on top of the glue pattern, where the positioning was done manually. Next, the other plate with glue was put over those to make a sandwich. The two carrier plates are joined using strips of Kapton to

prevent any slipping during the curing process. No external weights were applied during the curing process, apart from the weight of the top aluminium plate itself. The sample and the carrier plates were left to cure for 24 hours.

The description of the attachment of the silicon samples to the carrier plates that was used when manufacturing the samples is included in App. A.

2.1.4 Irradiation

All glues are expected to be radiation-hard, as specified by their manufacturers. The 3M tape has been tested by the NA62 experiment and is also radiation-hard. To measure any effects of radiation, half the samples were irradiated at the proton cyclotron at the University of Birmingham. They have been irradiated up to a fluence between 6 and 8×10^{15} MeV $n_{\text{eq}}/\text{cm}^2$. This is similar to the maximum expected fluence for the VeloPix sensors: 8×10^{15} MeV $n_{\text{eq}}/\text{cm}^2$ [1]. An overview of the exact irradiation per test sample is given in App. C.

2.2 Apparatus

A specially designed shear testing apparatus was used for the tests, fitted with force and distance sensors for data recording. A schematic diagram of the device can be seen in Figs. 4 and 5, where the main components of the device are labelled. The diagram shows the relative positioning of the sensors, the test sample compartment and the direction in which the force is applied. The tested sample is attached to aluminium carrier plates to which shear stress is applied via the load spring. The spring module can be detached and weights can be hung over the pulley to act as a load, which is used for the calibration of the force measuring load-cell and can also be used to apply larger forces. The position and load-cell sensors are connected to a computer for readout.

To hold the test samples in place and ensure that the shear load is applied uniformly, they need to be sandwiched between two larger aluminium plates before being placed in the sample compartment. The plates have the size of the compartment and allow for the secure positioning within the compartment via screws at both top and bottom plates of the compartment. The shear stress is applied to the sample by pulling tangentially on the carrier plates. The plates are positioned lying flat where the bottom one is held in place and the top one is allowed to move under the influence of an external force. The force can be applied both via a spring or with weights hanging over a pulley at the opposite end of the apparatus. To control the extension of the spring, a micrometer is provided that can push the far end of the spring precisely.

To quantify the adhesive response, the device is equipped with a position sensor for the top plate (LVDT) and a load cell to measure the external force applied. Both devices produce voltages that are proportional to the quantities they are measuring and are calibrated to obtain force and distance readings respectively. A diagram of the side-view of the apparatus is shown on Fig. 5, where the relative positions of the load-cell, LVDT and sample holder can clearly be seen.

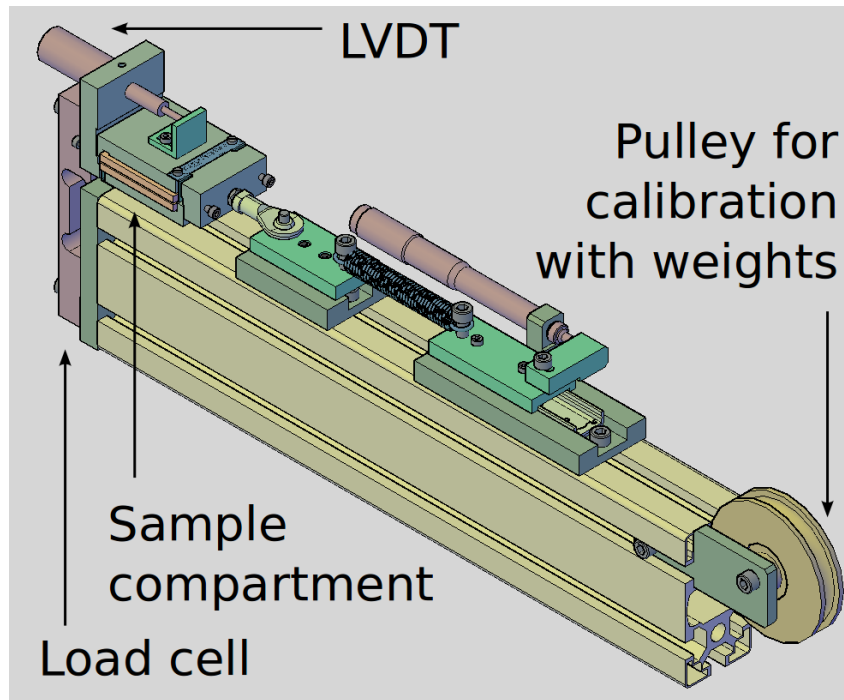


Figure 4: A schematic diagram of the shear testing apparatus with the main components labelled. The tested sample is attached to aluminium carrier plates (orange) to which shear stress is applied via the load spring. The spring module can be detached and weights can be hung over the pulley to act as a load. The shear force applied to the bottom plate is measured by the load cell, and the LVDT measures the displacement of the top carrier plate.

2.2.1 LVDT

A Linear Variable Differential Transducer (LVDT) is a device based on electromagnetic induction that accurately measures distances. It is comprised of three coils such that the centres of the coils are in a line and contain a cylindrical ferromagnetic core comprising the measuring tip. The central core is known as the primary energising coil with the two secondary ones on its sides. The tip of the LVDT is allowed to move along the central axis of the coils. To measure the displacement of the core, the primary coil is energised with an AC voltage. Depending on the position of the core relative to the two secondaries, the magnetic flux from the primary causes different electromotive force to be induced in the two secondary coils. The output voltage of the LVDT is given as the difference between the two secondaries which increases linearly with movement away from the equilibrium. The device used in the shear testing apparatus is a 10 mA Solartron Metrology Analogue Sensor (RS 646-482). The LVDT was powered by 10V DC from an external power supply. The output signal was read with a Keithley 2000 multimeter, which was connected to the computer over a RS-232 serial connection.

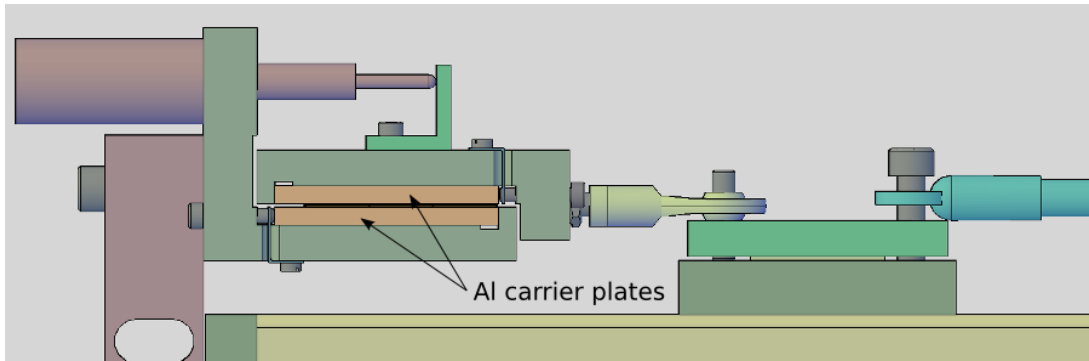


Figure 5: Side-view of the shear testing apparatus. The carrier plates (orange) are attached to both sides of the test sample and the bottom plate is held stationary via screws on both sides of the sample compartment. The LVDT is attached to measure the displacement of the top carrier plate, while the load cell measures the force on the bottom plate. Load is applied to the right via load cable using either spring or weights.

2.2.2 Load cell

A load cell is a mechanical to electrical transducer that is based on a strain gauge. It uses the piezo-electric properties of its active component and the change of its electric properties when deformed. When a load is applied to the cell, the gauge is deformed which can be measured by the change of its electrical resistance due to the change in its dimensions. By passing current through the gauge and making note of its resistance, the force applied to the cell can be accurately measured.

The shear testing apparatus was bundled with a Single Point Aluminium Load Cell Model 1022 manufactured by Tedeo-Huntleigh. The maximum operating load of the cell was found to be 100 N. Its readout was connected through a digital bridge amplifier (SY034). The amplifier was connected to the computer via USB interface from which it is also powered (5 V at 0.7 A).

2.3 Calibration

The calibration procedures for the load cell and LVDT are described in this section. In addition, a temperature correction has been applied due to the thermal expansion of the test samples. A summary of the calibration constants is shown in Table 2.

2.3.1 Load Cell Calibration

The load cell output was calibrated by the manufacturer. However, the absolute readout values were arbitrary and needed to be calibrated before they could be used to determine forces. A set of known loads were applied to the cell in order to establish the correspondence between readout units (LC units) and Newton. To determine this, the design of the testing

Sensor	Calibration coefficient
Load cell	61.21 mN/LC units
LVDT	-1.242 mm/V
Temperature	0.801 $\mu\text{m}/^\circ\text{C}$

Table 2: Summary of calibration results for two device sensors and the temperature correction. The calibration coefficient is the factor by which the sensor output needs to be multiplied to give the measured quantity in natural units.

device includes a pulley over which weights can be hung. When connected to the sample chamber these can replace the spring as a means of applying shear to the sample. Data was taken with increments of 200 g (1.96 N) from 0 to 80 N, where for each measurement the DAQ software was run to integrate the load-cell output for 60 s in order to produce a single mean reading with a standard deviation. The results of a linear fit $LC = mF + c$ and its residuals to the calibration measurements are shown in Fig. 6. F is the force applied, and m the inverse of the calibration constant.

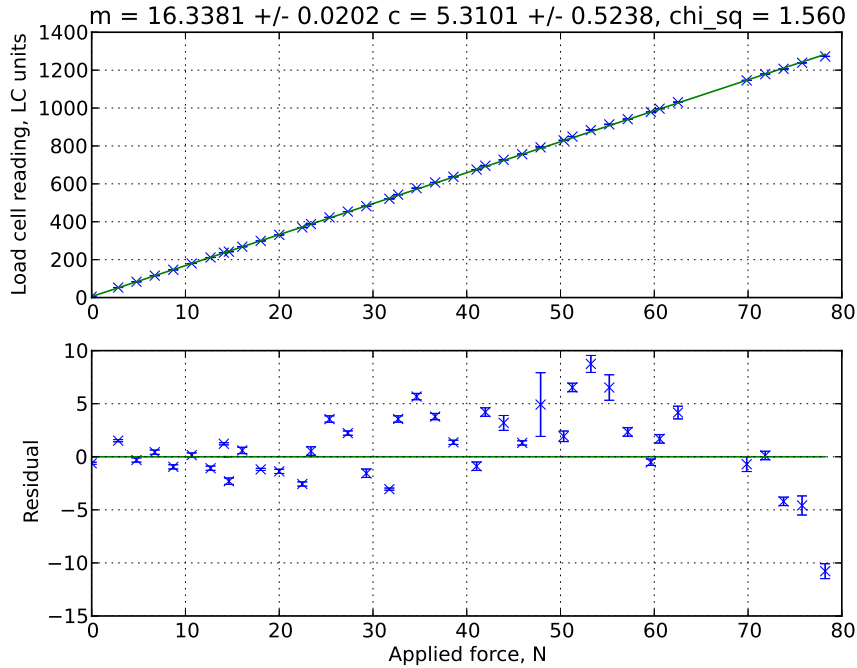


Figure 6: Results from a calibration measurement for load cell for conversion of load cell units (LC units) to Newton. The goodness of the fit is characterised by a reduced χ^2 of 1.56.

2.3.2 LVDT Calibration

The LVDT outputs a voltage proportional to the position of the cylindrical ferromagnetic core. The calibration was measured twice using a Newport SM-50 Vernier Micrometer graduated every 10 μm and a Keithley 2000 multimeter. Both measurements are in good agreement as is shown in Fig. 7, and reveals the linear dependence between the output voltage and the position of the ferromagnetic core with a correlation factor $R^2 > 0.9999$.

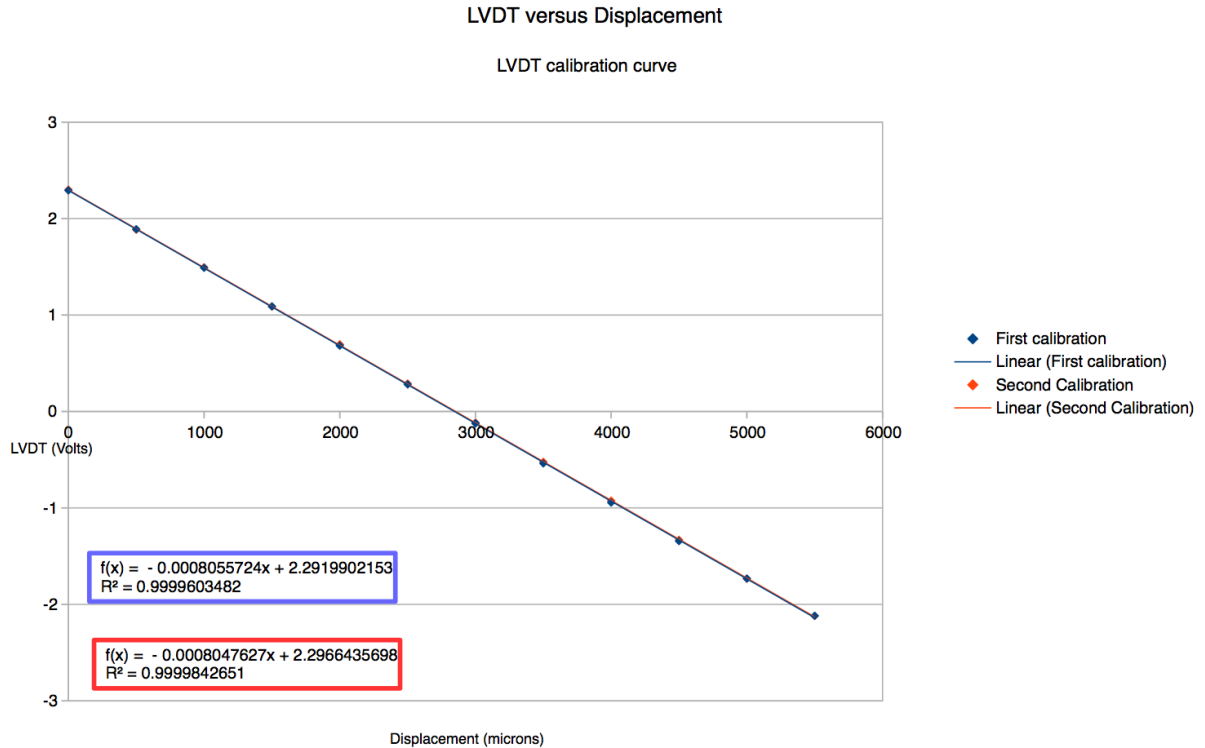


Figure 7: Results for calibration of the LVDT to convert Volts to microns.

2.3.3 Temperature Correction

The temperature in the lab varies between 17.5 and 22.5 $^{\circ}\text{C}$ over a 24 hour period. This causes the aluminium carrier plates to expand a measurable amount and this is corrected for. The distance between the back edge of the top plate and the left-most side of the sample is approximately 4 cm and changes due to the laboratory temperature. An extension of the apparatus of $\sim 0.8 \mu\text{m}/^{\circ}\text{C}$ is expected based on the thermal expansion coefficient of aluminium ($22.2 \times 10^{-6} \text{ m}/(\text{m}\cdot\text{K})$).

To measure the thermal coefficient of the shear test apparatus, a solid aluminium block was placed in the sample compartment. This block has the same thickness of the usual sample sandwich including the carrier plates. Data are taken over a period of two days. Before calibrating, data taken in periods where the temperature changes rapidly ($\sim 4 \text{ }^{\circ}\text{C}$ in

an hour) is removed. A non-linear least squares fit was performed to the data, see Fig. 8, which yields a temperature correction of: $0.801 \pm 0.002 \mu\text{m} / ^\circ\text{C}$. This is compatible with the expectation of $0.8 \mu\text{m} / ^\circ\text{C}$. It is also confirmed by the samples of Araldite that were tested, which showed no displacement.

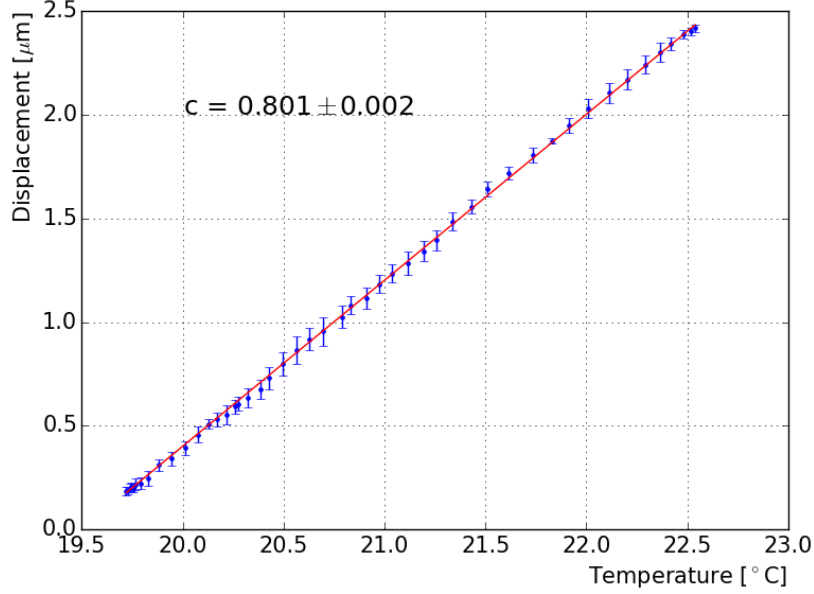


Figure 8: The displacement as a function of temperature using a solid aluminium block. This yields a temperature correction of: $\text{Displacement}[\mu\text{m}] = (0.801 \pm 0.002) \times T[^\circ\text{C}]$.

When the temperature fluctuates rapidly, the temperature correction for the displacement does not work sufficiently and it leaves spikes in otherwise flat graphs. Therefore, when the temperature fluctuates by more than $0.2 ^\circ\text{C}$ in two hours, the data has been removed from this analysis. This explains the gaps in the data shown in the results section. One of the days, the temperature in the lab fluctuated a lot, and for that day the temperature was allowed to vary by $0.5 ^\circ\text{C}$ in two hours. This is when sample S8 was tested.

2.4 Results

Of the five irradiated samples of each adhesive, three were dedicated to undergo the shear tests, while the others were reserved for thermal studies. The first of the three samples was to undergo all three tests, while the other two were dedicated for either the 10 N test, or others if deemed necessary. For Stycast, one additional sample was used because the previous three gave inconclusive results. The forces applied to the test samples are exerted by either a spring of force 0.1 N or 1.0 N, or a weight of 975 g, which roughly corresponds to 10 N. In addition, the LVDT contains a spring to push its metal rod against the setup in the same direction as the shear force is applied. This was determined to be of the order

of 0.5 N, such that the total forces exerted on the samples were 0.5, 1.5, and 10 N. The samples that have been tested are listed in Table 3. The description of the test procedure for the shear force testing is included in App. A.

Adhesive	Label	Weights tested [N]
Araldite 2011	A2	10
Araldite 2011	A6	10
Araldite 2011	A10	0.5; 1.5; 10
Stycast 2850FT	S2	10
Stycast 2850FT	S4	0.5
Stycast 2850FT	S7	0.5
Stycast 2850FT	S8	10
3M 9461P	3M2	0.5; 1.5; 10
3M 9461P	3M4	0.5
3M 9461P	3M6	0.5; 1.5; 10

Table 3: The samples that are tested and the force that was applied during the tests.

Araldite The Araldite samples show little to no displacement under any weight applied. This was expected and justifies assembling the carrier plates using Araldite. An overview of the displacement as a function of time of the three samples under a shear force of 10 N is shown in Fig. 9.

Stycast The Stycast samples proved to be rather fragile. Samples S4 and S7 were tested using 0.5 N and broke. Both of them broke after ~ 20 hours of testing, which is shown in Fig. 10. Two more Stycast samples (S2 and S8) were tested afterwards at 10 N. Both these samples stayed intact and show no displacement. A plot of the displacement versus time at 10 N is shown in Fig. 10. The large fluctuations in sample S8 can be explained by many rapid fluctuations in temperature. The usual removal of data with large temperature fluctuations could not be applied as almost all the data would be removed.

3M Tape One of the 3M samples (3M4) broke after removing it from the compartment holder after the 0.5 N test. The other two (3M2 and 3M6) have been tested over the full range and show minor displacement. Fig. 11 shows the results for the different forces applied. Because some samples showed increasing displacement over time, a longer test of 10 N over 35 days was performed for sample 3M6. The results of this are shown in Fig. 11 and show that the sample moves during the first week, before it stabilises and remains at a constant position.

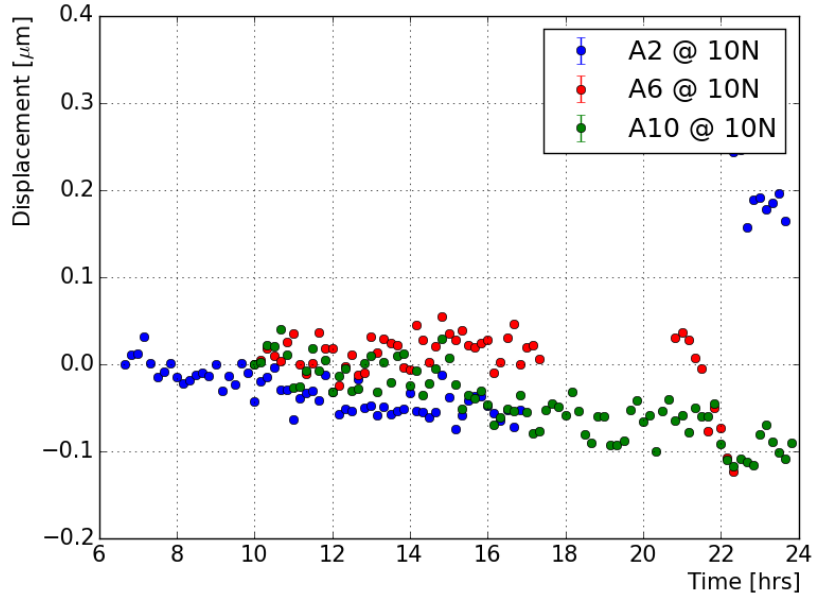


Figure 9: Displacement over time for the three Araldite samples tested at 10 N.

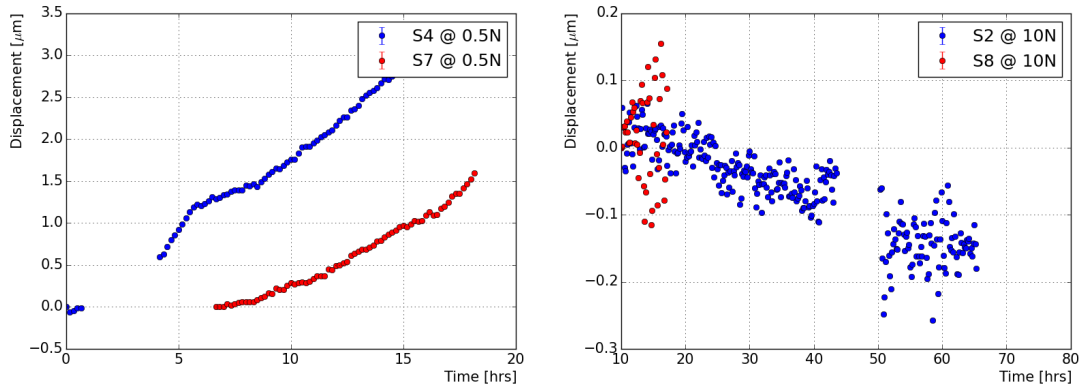


Figure 10: The displacement as a function of time for the Stycast samples. (Left) The samples that broke at a test of 0.5 N. (Right) the samples with a force of 10 N applied that show no displacement. The large fluctuation in sample S8 can be explained by the continuous rapid temperature change in the lab.

2.5 Notes on the Methods

There are several potential reasons for the breaking of some samples. When the Stycast samples break, usually all the glue residue is deposited on one side only, while the other silicon tile is clean. The samples that broke during the shear tests seemed to break during or after a rapid change of temperature. There is not, however, enough data to confirm this.

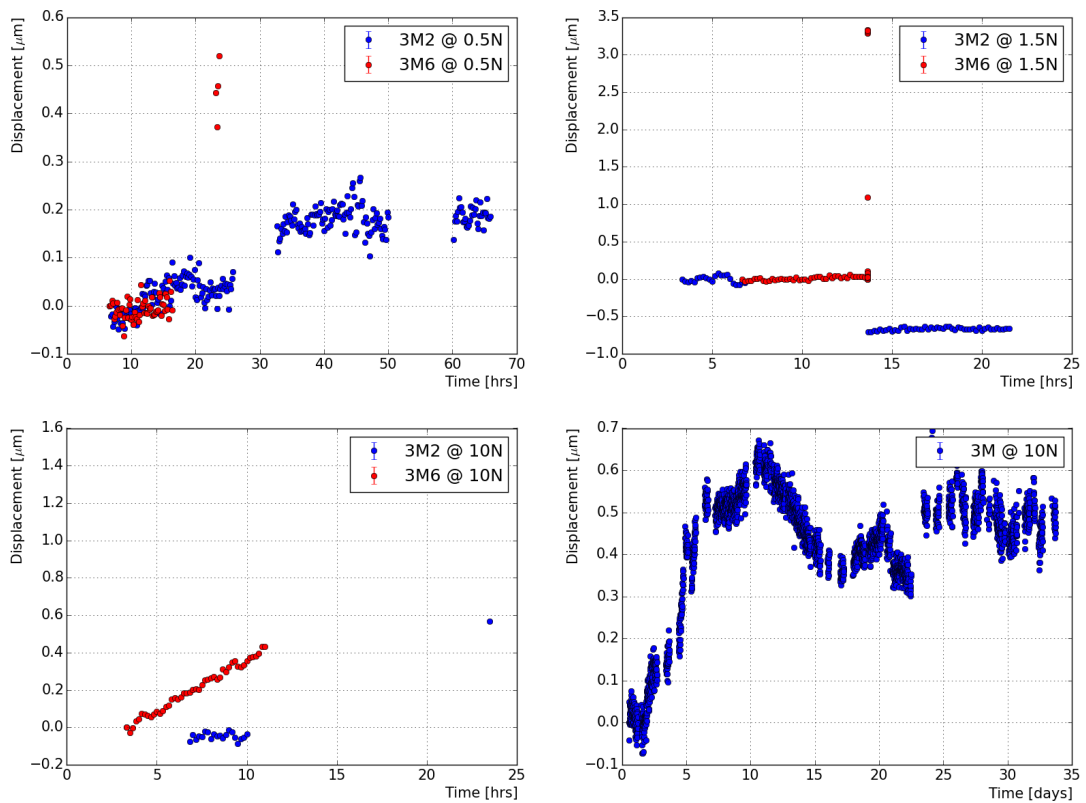


Figure 11: The results of the shear test for the 3M samples. (Top left) No displacement at 0.5 N. (Top right) Probably no displacement, as the jump for the 3M2 sample seems to be explained by an imperfect temperature correction. (Bottom left) An increasing displacement for one of the samples at 10 N. (Bottom right) An initial displacement, followed by stabilisation after a week for sample 3M6 tested at 10 N.

Moreover, it was noted that the alignment of the aluminium carrier plates is crucial. When these are slightly misaligned, this can exert a force when positioning them in the shear test apparatus. This could cause the samples to break and has been avoided as much as possible while producing the samples.

An interesting follow-up study could be a pattern with a mix of dots of Stycast and Araldite. This could make the samples less fragile, while keeping a high thermal conductivity.

3 Thermal studies

Directly measuring the thermal conductivity of the glues proved to be difficult and was attempted by using an infrared camera. Silicon is transparent to infrared, so the samples were covered by a non-reflective black paint in order to measure their temperature. This gave rise to a new problem: the black paint was less thermally conductive than the glues.

Therefore, a measurement of the relative thermal conductivity of the different glues studied is performed and compared with the manufacturer specifications.

3.1 Introduction

In the current setup the heat flow is perpendicular to the area of the samples. Under this condition we can use the Fourier's law that relates the heat transfer with the temperature gradient as follow:

$$\frac{\Delta Q}{\Delta t} = -A\sigma \frac{\Delta T}{\Delta x} \quad (1)$$

where $\Delta Q/\Delta t$ is the heat flow through a uniform material, A is the area, Δx is the thickness, σ is the thermal conductivity, and ΔT is the temperature difference across it. By setting the power conducted through two materials to be the same, and rearranging, the ratio of thermal conductivities can be obtained:

$$\frac{\sigma_1}{\sigma_2} = \frac{A_2 \Delta x_1 \Delta T_2}{A_1 \Delta x_2 \Delta T_1}. \quad (2)$$

This scenario is easily achieved in practice by applying the same heating power to each glue and waiting for a steady-state temperature difference to occur. Determining the thickness and area of the glue joint, and measuring the temperature difference across the joint allows a calculation of the ratio of thermal conductivities between the glues.

3.2 Test Setup

The test sample to perform these measurements consists of two small aluminium blocks, each of size $\sim 25 \times 9 \times 9$ mm³, as it is shown in Fig. 12. The aluminium blocks are attached to one another with the adhesive under test. Two PT100 temperature sensors are glued on the two free ends of the aluminium blocks to measure the temperature gradient. The setup is lying on a table while the tests are performed.

For the 3M tape, a single layer (30 ± 5 μm thick) is placed between the blocks and some pressure is applied briefly to produce a secure joint. For Araldite and Stycast, two strips of Kapton are attached to opposite edges of the gluing area to act as a spacer of 60 ± 5 μm thick. The area to be glued is measured to take into account that the regions covered by Kapton will not be glued. The glue is prepared and a small amount is placed on one block with a spatula; the two blocks are then pushed together firmly and the excess glue is wiped away. The bottom block is clamped in place vertically and a 20 g weight is placed on the top block. This is left for 24 hours to cure.

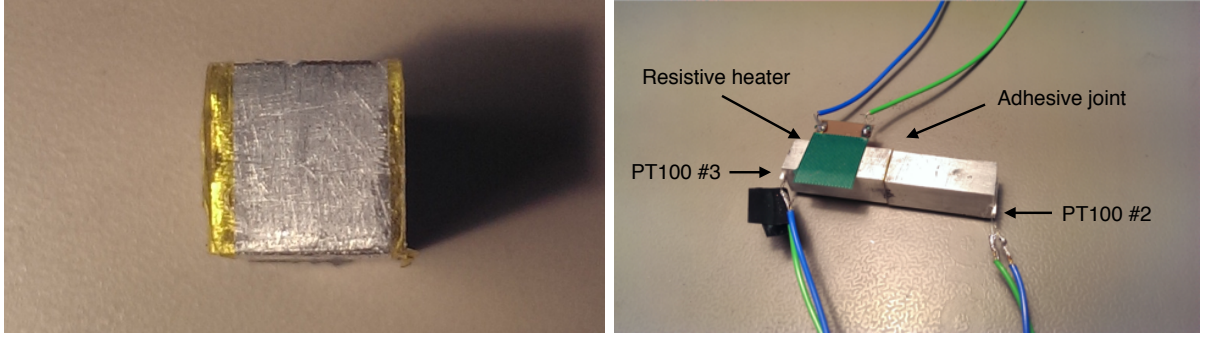


Figure 12: (Left) A picture of the aluminium block viewed from the surface where the glue will be deposited. Two narrow Kapton strips are attached on the edges of the aluminium block surface, used as a spacer to control the glue layer thickness. (Right) A picture of the two aluminium blocks glued together (the joint is where the black arrow points), with a heater glued onto one block and a temperature sensor (PT100) glued on each block.

The temperature sensors are readout by the Picolog recorder, and their values are shown in Fig. 13. As the PT100 use resistance to determine the temperature, equal lengths of wire are used to prevent a systematic shift in temperature reading between the sensors.

Finally, attached with 3M tape to the long side of one of the aluminium blocks is a 15×15 mm resistive heater. This is operated at a constant power of 1.5 V and ~ 0.5 A, which guarantees the constant 0.75 W heating power. The system is left for approximately one hour to reach a steady-state, after which the temperature is measured. This procedure was carried out for each glue, and the measurements are summarised in Table 4. The description of the test procedure used for carrying out these tests is included in App. B.

3.3 Results

A summary of the relative thermal conductivities and the comparisons with manufacturer specifications can be seen in Table 4. A correction for the area of the glues is used because parts of the area are covered by Kapton, which influences the total thermal conductivity. All relative results have been calculated relative to the 3M samples.

As the Kapton has lower thermal conductivity than the glues, a virtual area A' is calculated as follows:

$$A' = A_{Kapton} \cdot \frac{\sigma_{Kapton}}{\sigma_{glue}} \quad (3)$$

This area, A' , is added to the area that is covered by the glue, A_{adh} , to be the effective area A_{eff} : $A_{eff} = A_{adh} + A'$. The effective area is quoted in Table 4.

For the purposes of this correction, the thermal conductivities (σ) of Araldite, Stycast and Kapton are taken from the manufacturers data sheet [2, 3, 5]. Consequently, if the final results of the study are not in agreement with these values, an additional correction would be required.

Adhesive	A_{adh}/A_{3M}	σ_{spec} [W/m·K]	A_{eff}/A_{3M}	Δx [μm]	ΔT [$^{\circ}\text{C}$]	σ/σ_{3M}	$(\sigma/\sigma_{3M})_{spec}$
3M 9461P	1.00 ± 0.02	0.18 [4]	1.00 ± 0.02	30 ± 5	1.70 ± 0.06	1.00 ± 0.24	1.00
Stycast 2850FT	0.76 ± 0.02	1.12 [3]	0.79 ± 0.02	60 ± 5	0.85 ± 0.07	5.09 ± 1.07	6.22
Araldite 2011	0.80 ± 0.02	0.22 [2]	0.91 ± 0.02	60 ± 5	2.09 ± 0.10	1.79 ± 0.35	1.22
Kapton HN	-	0.12 [5]	-	60 ± 5	-	-	-

Table 4: Summary of thermal conductivity of three glues, as specified by their manufacturers, and the outcome of the relative thermal conductivities that were measured. The table also shows the relative area that the adhesives covered in the setup, A_{adh}/A_{3M} ; the relative effective area they covered, taking into account the thermal conductivity of Kapton, A_{eff}/A_{3M} ; the thickness of the adhesives, Δx ; and the temperature difference, ΔT .

The final results, adjusted for the conduction due to the Kapton are shown in Table 4. The errors on the thickness measurements are taken as 5 μm ; this is the resolution of the digital callipers used to measure the 3M and Kapton tapes; the measurements are compatible with the expected thicknesses. The calibration of the PT100s showed a systematic difference of 0.05 $^{\circ}\text{C}$ between the two channels which is assigned as an uncertainty.

The precision of PT100 sensors is dependent on the temperature; at 50 $^{\circ}\text{C}$ this is around 0.4 $^{\circ}\text{C}$. The sensors take a measurement every second, but the values used in the plots and calculations are the means of every minute of readings. The uncertainty on each point is the standard deviation of the readings in a minute.

The results in Table 4 confirm that Stycast is the best thermal conductor of the three glues and its relative conductivity to 3M is in line with the suggested values from the manufacturer. The Araldite appears to be a substantially better thermal conductor than the 3M tape, and possibly better than the manufacturer claimed. The results are close enough in agreement to justify the corrections that are made using the manufacturers specifications.

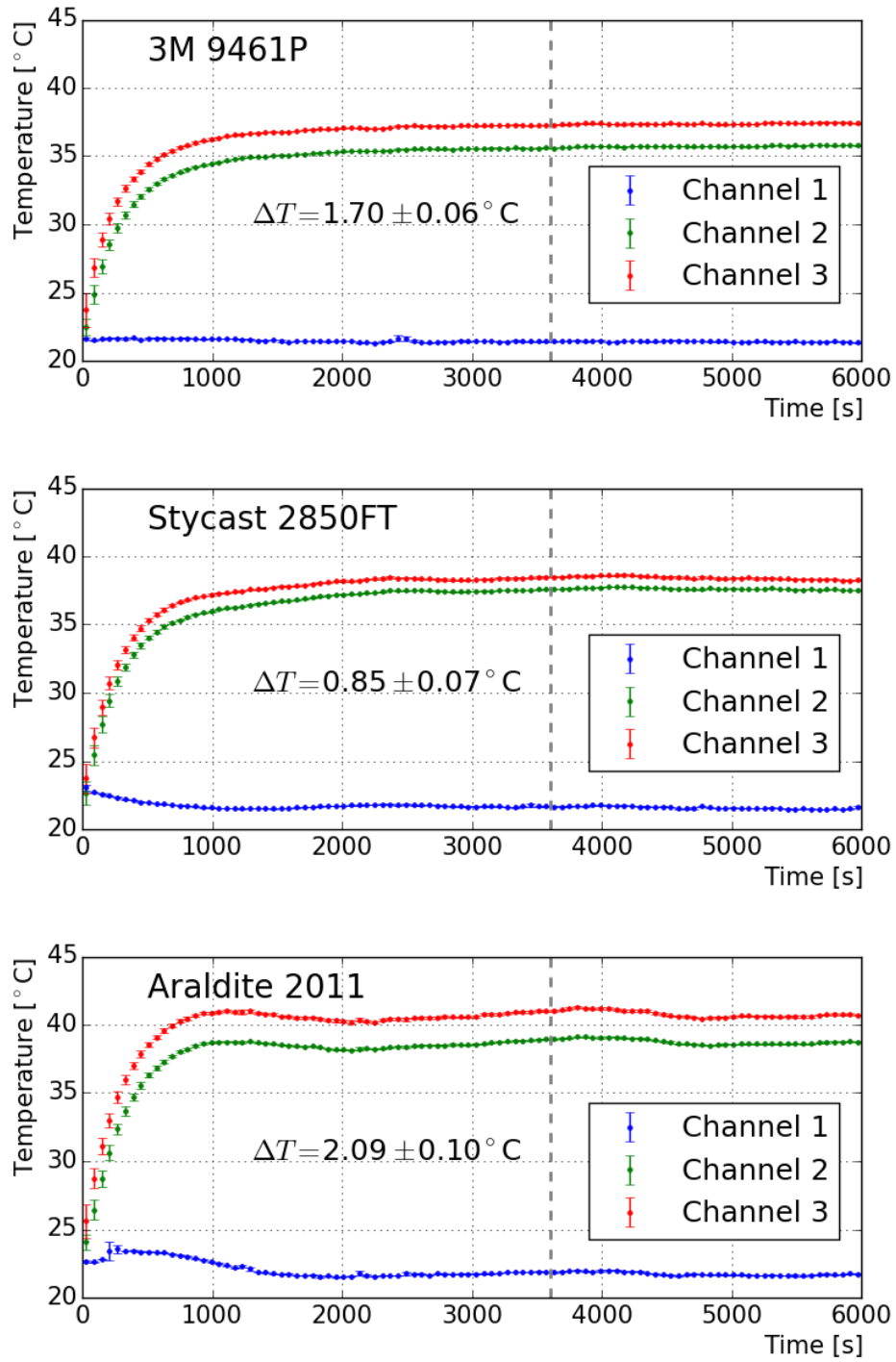


Figure 13: The temperature as a function of time of the three different adhesive samples. Channel 1 is the temperature of the air in the lab; channel 3 measures the temperature of the block with the heater attached and channel 3 the block without the heater. The temperature difference is measured after an hour, when the setup reached a stable temperature. This is indicated by the grey line.

4 Conclusions

This study has evaluated the thermal and mechanical performance of three adhesives. Irradiated samples of all three adhesives, Stycast 2850FT, Araldite 2011 and 3M 9461P have shown no displacement under a shear force of 10 N, which is more than sufficient for the VELO upgrade.

During the process of conducting different steps in the study, potential factors for improvement have been identified. If Stycast is utilised the fragility of the prototype modules should be studied or Araldite used in conjunction with it. For the 3M tape, leaving the samples under vacuum for several hours did not remove the tiny air bubbles that were trapped under the tape. Hence, a different method to remove those needs to be studied if this is to be used.

The thermal conductivities of the three adhesives are compatible with the specifications of their manufacturers. Stycast is approximately five times more conductive as the 3M tape, and Araldite is approximately twice as conductive as the 3M tape. The area that can be covered by the adhesives will be largest using the 3M tape, since that can cover the full area of the sensors. The areas of the glues can be studied only after the design of the glue pattern has been finalised such that no air bubbles will be trapped by the glue. It is estimated that the glues will cover approximately half the area of the 3M tape. This means that Stycast is still most conductive, while Araldite and 3M tape become comparable at the same glue layer thickness.

Appendices

A Shear force test procedure

This section gives an overview of the test procedure for determining the glue strengths.

A.1 Procedure for gluing samples

Procedure for gluing silicon samples to aluminium plates.

- If necessary to clean aluminium plates, use a heat gun and a scraper to remove any silicon still attached and rub with propanol to clean and degrease the plate.
- Prepare Araldite 2011 using a 1:1 (volume) mix of glue and hardener; stir slowly to avoid bubbles. Transfer into a syringe and push to the end with a stopper.
- On the glue robot, thread a rubber tube through the dispensing head, cut off any excess and insert the metal needle tip. Secure everything in place with screws.
- Screw the syringe into the dispensing head and attach the compressed air pipe, turn on the air supply and glue robot, check pressure ~ 4 bar. Press the switch to send compressed air until the glue starts coming out of the needle. Wipe off any excess with propanol on a rag and press switch once more.
- Set program to number 21 and place a degreased aluminium plate in the black guidelines in the robot and run the program.
- Run the program with a second aluminium plate and then secure the silicon tile between the plates using a 200 g weight on top and other weights to hold it square. Leave for 24 hours.

A.2 Procedure for shear force testing

There are three different adhesives that are tested: Araldite 2011, Stycast 2850 FT and 3M 9461P (tape). We take data for three weights on each glue to determine which weight gives the most useful data. The weights used are a spring, with an applied force of 0.1 N or 1 N, and a 975g (10 N) weight on a rope. Once it is determined which weight is most effective for which adhesive, this test is repeated twice more.

- Glue the sample between two aluminium plates as described above.
- Place the sample into the holder ensuring the plates are flush against each other. Tighten the screws to 25 Ncm with torque screwdriver.

- When applying 0.1 N or 1.0 N, retract the micrometer so the spring goes slack and make a note of the baseline force. Then extend the micrometer until the force reading has increased by the amount of force to be applied.
- When applying a 10 N load, remove the spring and micrometer from the apparatus. Then hang a 975 g weight from a piece of rope over the pulley, attaching it to the bolt that previously held the spring.
- Start the picolog software recording temperature readings every minute, then start logging the force and displacement data.
- Leave for ~ 24 hours and then stop the recording, on tests that run over a weekend we can just remove any data past 24 hours for consistency.
- Produce graphs using python scripts, correcting for temperature effects we have measured previously.
- Add the graphs and data sets to ELOG: <https://lhcbwiki.hep.manchester.ac.uk/VELO/>.

B Thermal test procedure

The procedure to carry out a test is as follows:

- Glue the aluminium blocks together, degreasing the surfaces with propanol.
- Set the power supply to output at 1.5 V, but do not turn it on.
- Connect the PT100s to the picolog recorder; a third PT100 is used to monitor the air temperature in the lab.
- Wait for the PT100s attached to the aluminium blocks to show similar readings close to that of the third. Then start recording the temperature at one second intervals and switch on the power supply.
- Leave the equipment for around 2 hours. Most of the first hour will be needed to allow the system to reach a steady-state, the time after that is to produce useful data.
- Calculate the average temperature difference between the two PT100s starting at 2000 seconds; starting at this point was found to give plenty of time for the apparatus to reach a steady-state.

C Specifications of the Irradiation

The specific conditions for every sample during the irradiation are given in Table 5 and Table 6. The irradiation took place at the Medical Physics MC40 cyclotron in the School of Physics and Astronomy at the University of Birmingham on two different days, labelled as Run I and II.

	Run I	Run II
Run Start	12:17	10:37
Run End	15:07	18:37
Run Length	165 min.	504 min.
Area of Foil	2.4 cm ²	2.4 cm ²
Faraday Cup	3821	12161
Measured Fluence	6.9964×10^{15}	22.267×10^{15}
Days Elapsed	8	7

Table 5: General conditions in both runs.

References

- [1] LHCb collaboration, *LHCb VELO Upgrade Technical Design Report*, CERN, Geneva, Switzerland, 2013.
- [2] Huntsman Advanced Materials, *Araldite 2011 Technical Data Sheet*, Switzerland, 2007.
- [3] Emerson and Cuming, *Stycast 2850FT Technical Data Sheet*, Belgium, 2001.
- [4] 3M, *3M High Temperature Acrylic Adhesive 100 Data Sheet*, USA, 2014.
- [5] DuPont, *Kapton HN Polyimide Film Technical Data Sheet*, Luxembourg, 2011.

Ni sample	Glue sample	Test time	Δt [min]	N_{iness}	rate [s^{-1}]	corr. rate [s^{-1}]	N at t_0 [s^{-1}]	Ni-57 produced	Fluence [$\times 10^{15}$ MeV $n_{\text{eq}}/\text{cm}^2$]	Total [$\times 10^{15}$ MeV $n_{\text{eq}}/\text{cm}^2$]
Run I										
C1	S9	10:21	11432	1490 \pm 48	1.49	9.21 $\times 10^3$	1.13 $\times 10^9$	6.97 $\times 10^{10}$	1.56 \pm 0.05	
C2	S8	10:39	11450	1420 \pm 45	1.42	8.77 $\times 10^3$	1.09 $\times 10^9$	6.69 $\times 10^{10}$	1.49 \pm 0.05	
C3	S7	11:08	11479	1439 \pm 47	1.439	8.89 $\times 10^3$	1.11 $\times 10^9$	6.84 $\times 10^{10}$	1.53 \pm 0.05	
C4	S4	11:26	11497	670 \pm 33	1.34	8.28 $\times 10^3$	1.04 $\times 10^9$	6.40 $\times 10^{10}$	1.43 \pm 0.07	
C5	S2	11:42	11513	711 \pm 31	1.422	8.79 $\times 10^3$	1.11 $\times 10^9$	6.83 $\times 10^{10}$	1.52 \pm 0.07	
D1	A10	11:51	11522	770 \pm 36	1.54	9.52 $\times 10^3$	1.20 $\times 10^9$	7.42 $\times 10^{10}$	1.65 \pm 0.08	
D2	A8	12:03	11534	862 \pm 37	1.724	1.07 $\times 10^4$	1.35 $\times 10^9$	8.34 $\times 10^{10}$	1.86 \pm 0.08	
D3	A6	12:12	11543	828 \pm 36	1.656	1.02 $\times 10^4$	1.30 $\times 10^9$	8.03 $\times 10^{10}$	1.79 \pm 0.08	
D4	A4	12:22	11553	876 \pm 36	1.752	1.08 $\times 10^4$	1.38 $\times 10^9$	8.53 $\times 10^{10}$	1.90 \pm 0.08	
D5	A2	12:32	11563	715 \pm 36	1.43	8.84 $\times 10^3$	1.13 $\times 10^9$	6.98 $\times 10^{10}$	1.56 \pm 0.08	
E1	3M11	12:41	11572	770 \pm 34	1.54	9.52 $\times 10^3$	1.22 $\times 10^9$	7.54 $\times 10^{10}$	1.68 \pm 0.07	
E2	3M8	12:50	11581	684 \pm 36	1.368	8.45 $\times 10^3$	1.09 $\times 10^9$	6.72 $\times 10^{10}$	1.50 \pm 0.08	
E3	3M6	12:59	11590	752 \pm 35	1.504	9.29 $\times 10^3$	1.20 $\times 10^9$	7.41 $\times 10^{10}$	1.65 \pm 0.08	
E4	3M4	13:08	11599	706 \pm 34	1.412	8.73 $\times 10^3$	1.13 $\times 10^9$	6.97 $\times 10^{10}$	1.56 \pm 0.07	
E5	3M2	13:17	11608	761 \pm 34	1.522	9.40 $\times 10^3$	1.22 $\times 10^9$	7.54 $\times 10^{10}$	1.68 \pm 0.08	
Run II										
F1	S9	14:43	10254	1924 \pm 51	6.413	3.96 $\times 10^4$	3.34 $\times 10^9$	2.17 $\times 10^{11}$	4.84 \pm 0.13	6.39
F2	S8	14:50	10261	2239 \pm 51	7.463	4.61 $\times 10^4$	3.89 $\times 10^9$	2.53 $\times 10^{11}$	5.64 \pm 0.13	7.13
F3	S7	14:56	10267	1588 \pm 46	6.352	3.93 $\times 10^4$	3.32 $\times 10^9$	2.16 $\times 10^{11}$	4.81 \pm 0.14	6.33
F4	S4	15:01	10272	1565 \pm 46	6.26	3.87 $\times 10^4$	3.27 $\times 10^9$	2.13 $\times 10^{11}$	4.75 \pm 0.14	6.18
F5	S2	15:06	10277	1583 \pm 42	6.332	3.91 $\times 10^4$	3.32 $\times 10^9$	2.16 $\times 10^{11}$	4.81 \pm 0.13	6.33
G1	A10	15:11	10282	2036 \pm 51	8.144	5.03 $\times 10^4$	4.27 $\times 10^9$	2.78 $\times 10^{11}$	6.20 \pm 0.16	7.85
G2	A8	15:16	10287	2108 \pm 55	8.432	5.21 $\times 10^4$	4.43 $\times 10^9$	2.88 $\times 10^{11}$	6.43 \pm 0.17	8.29
G3	A6	15:21	10292	2097 \pm 46	8.388	5.18 $\times 10^4$	4.42 $\times 10^9$	2.87 $\times 10^{11}$	6.40 \pm 0.14	8.19
G4	A4	15:26	10297	2060 \pm 55	8.24	5.09 $\times 10^4$	4.35 $\times 10^9$	2.82 $\times 10^{11}$	6.30 \pm 0.17	8.20
G5	A2	15:31	10302	1980 \pm 51	7.92	4.89 $\times 10^4$	4.18 $\times 10^9$	2.72 $\times 10^{11}$	6.06 \pm 0.16	7.62
H1	3M11	15:37	10308	1861 \pm 51	7.444	4.60 $\times 10^4$	3.94 $\times 10^9$	2.56 $\times 10^{11}$	5.71 \pm 0.16	7.39
H2	3M8	15:42	10313	2027 \pm 66	8.108	5.01 $\times 10^4$	4.30 $\times 10^9$	2.79 $\times 10^{11}$	6.23 \pm 0.20	7.73
H3	3M6	15:46	10317	2098 \pm 50	8.392	5.19 $\times 10^4$	4.45 $\times 10^9$	2.89 $\times 10^{11}$	6.46 \pm 0.15	8.11
H4	3M4	15:51	10322	1993 \pm 52	7.972	4.93 $\times 10^4$	4.24 $\times 10^9$	2.75 $\times 10^{11}$	6.14 \pm 0.16	7.70
H5	3M2	15:57	10328	1965 \pm 54	7.86	4.86 $\times 10^4$	4.19 $\times 10^9$	2.72 $\times 10^{11}$	6.07 \pm 0.17	7.75

Table 6: The fluence and other radiation specifics per test sample.